

Article

Pest animal's Detection, and Habitat Identification in Low-resolution Airborne Thermal Imagery

Anwaar Ulhaq ^{1,†,‡,*}, Peter Adam ^{2,‡}, Tarnya Cox ^{3,‡}, Asim Khan ^{4,‡}, Tom Low ^{5,‡} and Manoranjan Paul ¹

¹ School of Computing and Mathematics, Charles Sturt University, NSW, Australia;

² Department of Primary Industries and Regional Development, WA, Australia; peter.adams@dpird.wa.gov.au

³ Department of Primary Industries , NSW, Australia; tarnya.cox@dpi.nsw.gov.au

⁴ Victoria University, Melbourne, VIC, Australia; asim.khan@vu.edu.au

⁵ Tomcat Technologies, Australia; tom@kargow.com

* Correspondence: aulhaq@csu.edu.a

Version September 21, 2020 submitted to Preprints

1 **Abstract:** Invasive species are significant threats to global agriculture and food security being the major causes
2 of crop loss. An operative biosecurity policy requires full automation of detection and habitat identification of
3 the potential pests and pathogens. Unmanned Aerial Vehicles (UAVs) mounted thermal imaging cameras can
4 observe and detect pest animals and their habitats, and estimate their population size around the clock. However,
5 their effectiveness becomes limited due to manual detection of cryptic species in hours of captured flight videos,
6 failure in habitat disclosure and the requirement of expensive high-resolution cameras. Therefore, the cost and
7 efficiency trade-off often restricts the use of these systems. In this paper, we present an invasive animal species
8 detection system that uses cost-effectiveness of consumer-level cameras while harnessing the power of transfer
9 learning and an optimised small object detection algorithm. Our proposed optimised object detection algorithm
10 named Optimised YOLO (OYOLO) enhances YOLO (You Only Look Once) [27] by improving its training and
11 structure for remote detection of elusive targets. Our system, trained on the massive data collected from New
12 South Wales and Western Australia, can detect invasive species (rabbits, Kangaroos and pigs) in real-time with
13 a higher probability of detection (85–100 %), compared to the manual detection. This work will enhance the
14 visual analysis of pest species while performing well on low, medium and high-resolution thermal imagery, and
15 equally accessible to all stakeholders and end-users in Australia via a public cloud.

16 **Keywords:** invasive species; thermal imaging; habitat identification; deep learning

17 1. Introduction

18 A pest animal is defined as any animal that has or has the potential to have an adverse economic,
19 environmental or social/cultural impact [8]. Pest animals have adverse effects on Australian agri-ecosystem
20 as they cause significant crop damage, competing with native species for pasture or causing soil erosion, and
21 acting as reservoirs for diseases. Invasive population expansion of European rabbit (*Oryctolagus cuniculus*) and
22 Feral pig (*Sus scrofa*) are among the more pervasive invasions to crops and agricultural lands. The kangaroo
23 (Macropodidae) is a symbol of Australia and not considered a pest [13]. However, they are involved in more
24 than eighty per cent of the 20,000-plus vehicle-animal collisions reported each year [14]. Rabbit-proof fencing,
25 ground and helicopter culling of pigs and Kangaroos, pest trapping and poisoning, are some of the control
26 strategies in place. However, the pest population is rapidly spreading despite substantial investment in control.

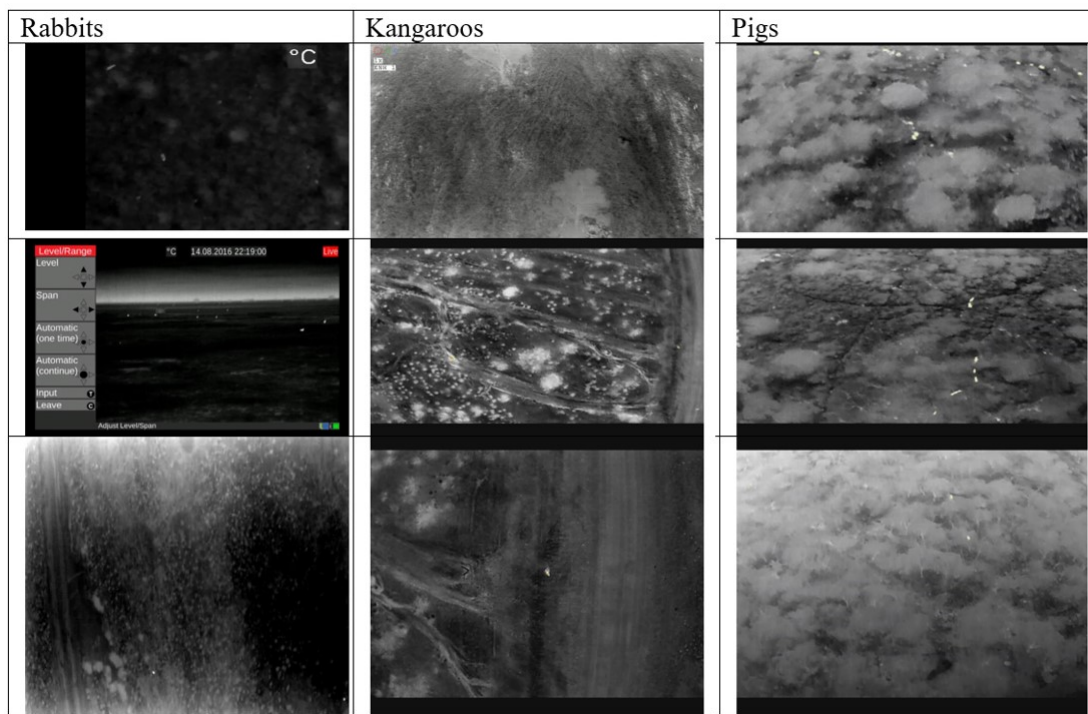


Figure 1. An exemplar shots of dataset shots of invasive animals (rabbits, pigs and Kangaroos) captured in airborne thermal imagery that show visual challenges for object recognition from a distance. These videos are captured using helicopter-based surveys of vast farmlands in states of Western Australia (WA) and New South Wales (NSW), Australia.

Recent advancements in drone and imaging technologies have enabled non-invasive monitoring of pest animals [4,10,18,32]. However, manual detection of pest animals, habitat identification and estimation of pest population size is cumbersome as it requires frame by frame analysis of hours of video data. Some automated approaches are proposed in recent years [2,6,19,25,31]. However, they often lack usability due to low accuracy, ineffectiveness against occlusion, limitations of the visible spectrum and low detection speed. It requires a need for an intelligent, real-time, fully automated and around the clock monitoring system that is not only limited to animal detection but also their habitat identification. Thermal imagery can provide crucial information about animal habitats that look more active and warm in thermal heat maps.

However, such approaches work better for large mammals as the drastic changes in the temperature gradient between mammals, and their cold background can distinguish their thermal signatures, facilitating their detection and count. In the pest animal remote sensing scenario, both small and elusive signatures are available that decrease the accuracy of computer vision algorithms. Figure 1 shows some dataset shots of invasive animals (rabbits, pigs and Kangaroos) captured in airborne thermal imagery that show visual challenges for object recognition from a distance. As object size becomes very small, even manual identification and tagging of correct thermal signatures is problematic.

Deep learning has revolutionised the field of object detection, and various deep object detection approaches exist in the literature. Some of the notable techniques include RCNN [12], Fast-RCNN [11], Faster-RCNN [29], Mask-RCNN [16], FPN [20], SSD [23] and YOLO [27]. RCNN family of detectors are two-stage detectors based on the concept of region proposals requiring considerable processing time and unsuitable for fast and real-time object detection. SSD (single-shot multibox detector) and YOLO (You Only Look Once) are one stage or one-shot detectors. SSD is very slow for detection tasks due to the sliding window approach while YOLO outperforms these approaches in both accuracy and processing time. As YOLO initially is trained on MS COCO dataset [21], its performance suffers if objects are tiny and receptive field is limited. YOLOv3 [28] uses DarkNet-53 for feature extraction and introduces the Feature Pyramid to detect small objects at different

51 scales. FPN predicts small-scale objects in the shallower layers with low semantic information which might not
52 be sufficient to classify small objects.

53 Similarly, due to striding and pooling, the small-scale objects disappear in the deep convolution layers.
54 Therefore, the removal of pooling and striding can improve YOLO to detect smaller objects. Meanwhile,
55 YOLOv4 [3] presents new findings. However, its scope is to increase the overall speed and accuracy on MS
56 COCO dataset using a different bag of features and bot to increase small object detection in thermal imaging.
57 In this work, we address the above weaknesses by introducing an optimised version of YOLO for small object
58 detection. We named it Optimised YOLO. It enables us to propose a real-time pest animal detection with
59 improved accuracy on imagery captured from consumer-level thermal cameras counted on an unmanned aerial
60 vehicle.

61 We claim the following contributions in this paper:

62 • We introduce a real-time pest animal detection with improved accuracy and speed using deep learning-based
63 small object detection approach.
64 • We optimise traditional YOLO by improved model training and structure optimisation for detecting smaller
65 objects.
66 • We validate our approach on an extensive thermal video data set collected by the Department of Primary
67 Industries, NSW, Australia. This dataset is very challenging due to low resolution, the small size of pets
68 like rabbits and elusive signatures of similar thermals signatures of pigs and Kangaroos.

69 We have organised the paper as follow: Section 2 describes the related work. Section 3 provides a detailed
70 description of our methodology. Section 4 illustrates our finding with the help of experimental results. Section 5
71 presents the discussion and future work directions, followed by concluding remarks and references.

72 2. Related Work

73 One of the traditional approaches to animal detection and activity monitoring is the use of camera traps.
74 They have been used to investigate 13 broad areas of wildlife monitoring in Australia over the last twenty-four
75 years [24?]. However, the field of view and coverage of camera traps is limited, and it has not proved to be a
76 reliable tool to monitor cryptic pest animals and their activities[33]. An alternative way to airborne monitoring
77 through unmanned aerial vehicles (UAVs) and helicopters [1,4,9,10,18,32].

78 The recent revolution in the field of deep learning [30] has enabled scientists to automate various
79 vision-based problems. Early use of deep learning for automated animal classification involved sufficient
80 pre-processing and limited recognition accuracy [5,7]. Domain adaptation and transfer learning [19] can increase
81 detection accuracy across different domain and tasks.

82 Animal detection work can also be categories can object detection problem as there is more interest in
83 object recognition and location detection than in simple classification. Various object detection methodologies
84 can be used that include RCNN [12], Fast-RCNN [11], Faster-RCNN[29], Mask-RCNN [16], FPN [20], SSD
85 [23] and YOLO [27]. However, all these approaches use high-resolution data for training and object scales
86 are generally larger and clear. Therefore, their performance decreases for small animal detection from UAV,
87 especially in low-resolution thermal video sequences resulting in low accuracy, slow detection or overfitting.

88 Our work is related to YOLO YOLO [27] and its improved versions [3,28]. Some recent work on small
89 object detection from a distance is related to our work. An improved version of YOLO for UAV called UAV-YOLO
90 [22] tried to improve small object detection through YOLO. It has included a few more convolution layers and
91 shortcut connections to improve the model. However, the basic limitations of subsampling remain unaddressed. In
92 this work, we addressed the major weakness of convolution operation and aggressive subsampling and proposed
93 an optimised YOLO.

94 3. Materials and Methodology

95 In this paper, we used the Convolutional neural network (CNN)-based object detection method for pest
96 animal detection in thermal imaging. Data collection. In order to perform this study, we first established the
97 Australian pest animal database that was collected by two different teams. One team from the department

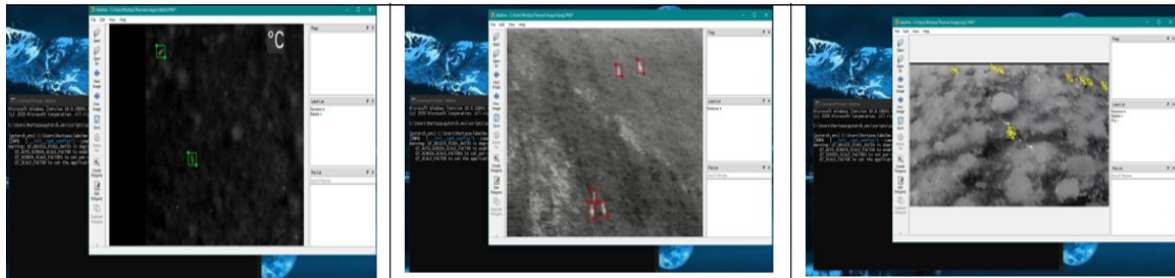


Figure 2. Data annotation samples for different pest species in our pest dataset.

98 of primary industry, NSW was responsible for the collection of rabbit movement and warren footage using
 99 helicopter-based surveys. The other team at Department of primary industry and regional development, Western
 100 Australia was responsible for data collection related to wild pigs and Kangaroos using drones.

101 *3.1. Data collection and Annotation*

102 In order to perform this study, we first established the Australian pest animal database that was collected by
 103 two different teams. One team from the department of primary industry, NSW was responsible for the collection
 104 of rabbit movement and warren footage using helicopter-based surveys. The other team at Department of primary
 105 industry and regional development, Western Australia was responsible for data collection related to wild pigs and
 106 Kangaroos using drones.

107 From the thermal footage, we extracted frames to prepare training dataset. As the video framerate 60fps, so
 108 thus we had a huge number of frames. However, the majority of frames has no evidence of the presence of any
 109 invasive animals; we used only those frames that had confirmed the presence of targeted pest animals.

110 We manually labelled the dataset. We used python based library Labelme, which is a graphical image
 111 annotation tool inspired by <http://labelme.csail.mit.edu>. We also observed that target objects were very small in
 112 some of the frames that had been collected from a high altitude. Similarly, some of the targets were obscure, and
 113 even manual classification of their thermal signatures was challenging. We had to magnify such frames/images to
 114 label them accurately. Some sample shots of the manual annotation of our thermal dataset are shown in Figure 2.

Table 1. Dataset used for training purpose

Class Name	Labeled	Total Images
Rabbit	Rabbit	1246
Kangaroos	Kangaroo	4211
Pigs	Pig	6000

115 *3.2. Pest Animal Annotation, Model Training and Detection*

116 Our footage library was extensive, so we divided it into three groups of datasets: training dataset, evaluation
 117 dataset and testing dataset. We annotated interested target pest animals in our training dataset using Python-based
 118 annotation tool. We then trained our proposed OYOLO (Optimised You Look Only Once) model on the trained
 119 dataset. The detailed description of OYOLO is provided in coming subsections.

120 During data collection, our crew took both far and nearer footage of animals by different camera zoom.
 121 Therefore, to optimise the performance of YOLOv3 for small object detection, we divided our dataset into two
 122 categories named “zoom in”, “zoom-out” groups by taking the distance and receptive field in consideration. We
 123 also used data augmentation to balance their sizes. k-means [15] is then used to cluster different numbers of
 124 anchor boxes to find the optimised number and size for better results. Finally, the model is retrained by zoom
 125 out-category data. On the other hand, the backbone structure of YOLO3 is improved to improve performance.

126 **A brief introduction to YOLO:**

127 YOLOv3 is a more established one-shot detector that is an incremental model of the former YOLO[26] and
 128 YOLO9000 [27] and deals object detection as a regression problem.

129 YOLOv3 backbone known as Darknet 53 includes 53 convolution layers and Resnet [17] short cut
 130 connections. In the prediction stage, it uses FPN (Feature Pyramid Network) that uses three scale feature
 131 maps, where small feature maps provide semantic information, and large feature maps provide finer-grained
 132 information. YOLOv3 uses independent logistic classifiers rather than softmax with binary cross-entropy loss
 133 for the class predictions in the training stage. FPN uses three scales of detection with different receptive fields,
 134 where the 32-fold downsampling is suitable for large objects, the 16-fold for middle size objects, and the 8-fold
 135 for small size objects.

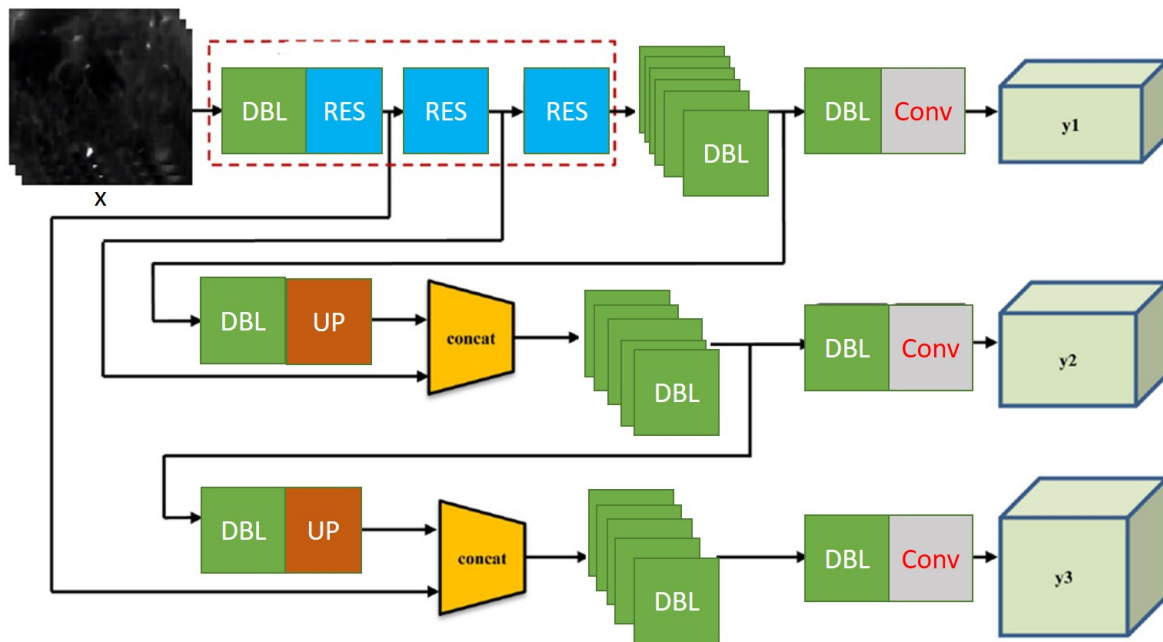


Figure 3. YOLOv3 architecture with input image size 416 x 416 and 3 types of feature map (13 x 13 x 3, 26 x 26 x 3 and 52 x 52 x 3) as output; (B) DBL is Darknet conv2D BN Leaky composed of one convolution layer, one batch normalisation layer and one leaky relu layer.; ResUnit includes two "DBL" structures followed by one "add" layer leads to the residual-like unit, "ResBlock" has several "ResUnit" with one zero-padding layer and "DBL" structure forward generates a residual-like block, "ResBlock." is the module element of Darknet-53.

136 An architectural diagram of YOLOv3 is shown in Figure 3 that takes an input image size 416 x 416 and
 137 3 types of feature map (13 x 13 x 3, 26 x 26 x 3 and 52 x 52 x 3) as output; (B) DBL is Darknet conv2D BN
 138 Leaky composed of one convolution layer, one batch normalisation layer and one leaky relu layer.; ResUnit
 139 includes two "DBL" structures followed by one "add" layer leads to the residual-like unit, "ResBlock" has several
 140 "ResUnit" with one zero-padding layer and "DBL" structure forward generates a residual-like block, "ResBlock."
 141 is the module element of Darknet 53. This architecture is shown in Figure 2.

142 **YOLO: The optimised YOLO:**

143 One of the problems with traditional CNN networks is their inability to handle low resolution and receptive
 144 field as both pooling and striding may cause loss of small targets. The semantic information about the small
 145 objects will vanish or weaken with a decreased spatial resolution of feature maps in subsequent layers. Low
 146 semantic information may not be enough to recognise the small object category in thermal images.

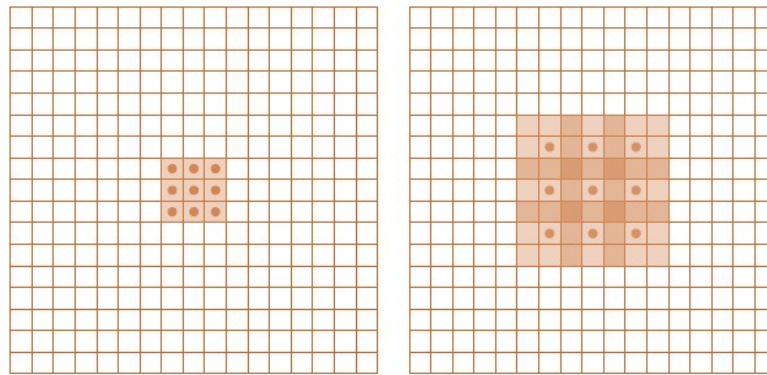


Figure 4. Dilated Convolutions: Figure 3(A) on left shows F_2 that is generated from F_1 by a 1-dilated convolution; each element in F_2 has a receptive field of 3×3 . Figure 3(B) on right shows F_3 that is generated from F_2 by a 2-dilated convolution; each element in F_3 has a receptive field of 7×7 .

147 A region of the input on which a pixel value in the output depends on is called the receptive field. CNN's
 148 progressive reduce resolution and removing subsampling can help, but it reduces the receptive field. Dilated
 149 convolutions [34] can increase the resolution of the output feature maps without harming the receptive field of
 150 individual neurons. Dilated convolution is also called as "convolution with a dilated filter" as it is a similar filter
 151 that is used for wavelet transformation. This concept is explained in Figure 4.

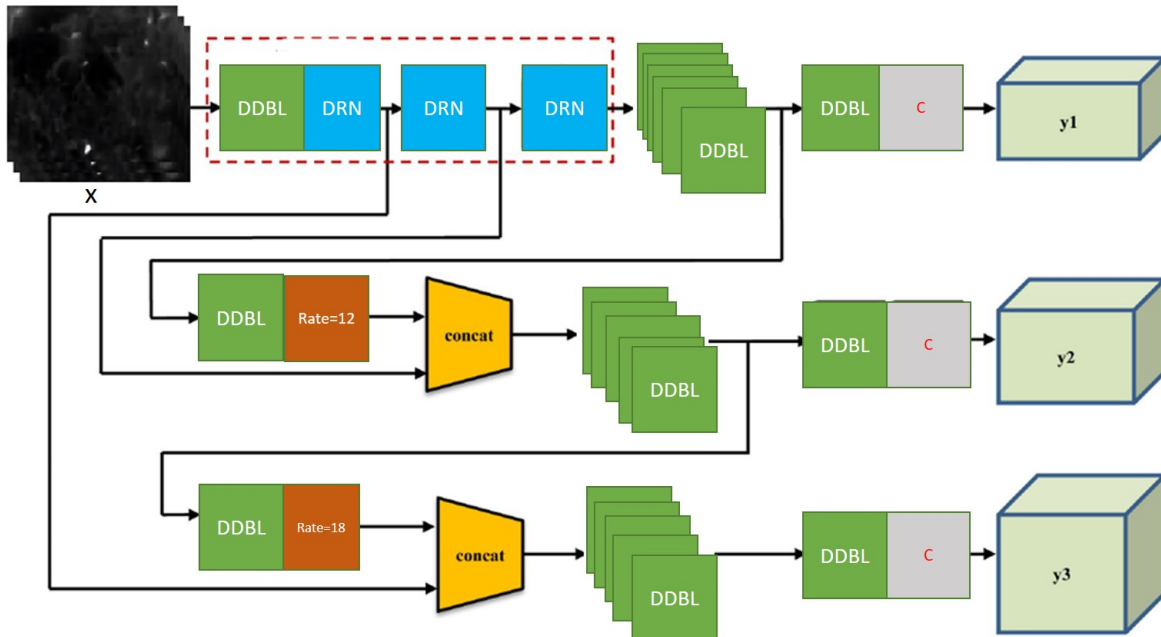


Figure 5. OYOLO architecture with input image size 416×416 and 3 types of feature map ($13 \times 13 \times 3$, $26 \times 26 \times 3$ and $52 \times 52 \times 3$) as output; (B) DDBL is Darknet dilated conv2D BN Leaky composed of one convolution layer, one batch normalisation layer and one leaky relu layer.; DRN (Dilated Residual Network) provides residual like connection with dilated convolutions. Similarly, for multiscale spatial pooling, we use different dilation rates and replace upsampling with dilation filtering.

152 Let $F : \mathbb{Z}^2 \rightarrow \mathbb{R}$ is a discrete function, $\Phi_n = [-n, n]^2$ and let $f = \Phi_n \rightarrow \mathbb{R}$ is another discrete, the convolution
 153 operator $*$ can be defined as :

$$(F * f)(x) = \sum_{s+t=x} F(s)f(t) \quad (1)$$

154 Let d be a dilation factor and let $*_d$ be defined as:

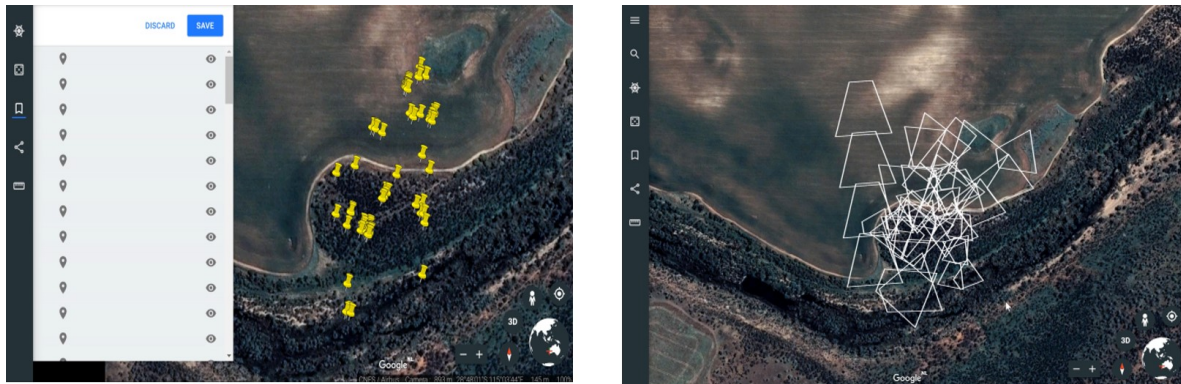


Figure 6. (A) The geo-tagging of detected pest animals from drone data that points out their detection location and (B) visualisation of pest movements that display the area of their activity.

$$(F *_d f)(x) = \sum_{s + *_d t = x} F(s)f(t) \quad (2)$$

155 where $*_d$ is a dilated convolution or a d-dilated convolution. The tradition CNN convolution is simply the
 156 1-dilated convolution. Dilated convolution supports an exponential expansion of the receptive field without loss
 157 of resolution—figure 3 illustrated outcome of dilated convolution. Figure 3(A) shows F2 that is generated from
 158 F1 by a 1-dilated convolution; each element in F2 has a receptive field of 3×3 . Figure 3(B) shows F3 that is
 159 generated from F2 by a 2-dilated convolution; each element in F3 has a receptive field of 7×7 .

160 Therefore, to increase the receptive field of YOLO to handle small objects, we integrated dilated convolutions
 161 in its architecture. For this purpose, we replaced DDL block with DDDL block that uses dilated convolution
 162 followed by batch normalisation and leaky Relu. RES block is replaced with DRN (Dilated Residual Network)
 163 [35]. Similarly, for multiscale spatial pooling, we use different dilation rates and replace upsampling with dilation
 164 filtering. Finally, semantic information from three scales is concatenated to detect objects and their categories.
 165 Optimised YOLO architecture is shown in Figure 5.

166 *3.3. Geo-tagging and Visualizing of Detected Targets:*

167 Finally, geo-tagging of detected pest animals is done by embedding Google maps platform done flight
 168 GPS data for locating and visualising targets in real-time. It provides precise tracking of target locations and
 169 visualisation of their movement within the surrounding. Such information is key to monitor pest animal movement
 170 patterns and valuable insight about their activities. Figure 6 illustrates the process of geo-tagging of detected pest
 171 animals from drone data and also provides visualisation of their movements during the time of flight.

172 *3.4. Results*

173 In this section, we describe the description of our image dataset, system parameters, list of experiments and
 174 their results. We would also discuss our experimental results and future work directions.

175 Two different teams collected our thermal image dataset. One team from the department of primary industry,
 176 NSW was responsible for the collection of rabbit movement and warren footage using helicopter-based surveys.
 177 The other team at Department of primary industry and regional development, Western Australia was responsible
 178 for data collection related to wild pigs and Kangaroos using drones.

179 Platform specifications: One of our team used DJI Matrice 210 drone with DJI Zenmuse XT (thermal)
 180 cameras of 640×512 resolution, 9 Hz collected footage at 60 fps. This flying time (with each flight 5-6 hours)
 181 is all during night footage was collected. Each 12-15 min length file is approximately 250 MB. This survey
 182 included rabbits, pigs and Kangaroos and flight area covered farmlands in Western Australia. At the same time,
 183 the other team collected footage of rabbits and their warrens using a helicopter-based thermal imaging platform
 184 for farmlands in New South Wales, Australia. Our helicopter crew used (DJI M600 and old footage from DJI

185 S1000 and DJI Inspire 2) Camera is Vayu HD by Sierra Olympic with a flight time of 3-5 hours for drone and,
 186 10-15 for helicopter: The size of the collected video was around 3 TB.

Table 2. System Specifications for Training/Testing

System Hardware / Software (Operating System)	Specifications
RAM	64 GB RAM
CPU	Intel 9th Gen i9 9900K
GPU(s)	2x NVIDIA RTX 2080 Ti 11 GB VRAM
Operating System	Windows 10 Professional and Ubuntu 18.04

187 The whole dataset was divided into training and validation as 85% and 15% respectively, as shown in the
 188 table 7 to get the optimised results and overcome the issue of over-fitting. For our deep model, we carried out the
 189 training process, experiments both on Windows and Ubuntu operating systems. We used deep learning framework
 190 PyTorch and related Python libraries for system training and testing. Training and testing were performed on
 191 both windows and ubuntu operating systems workstation. It had intel ninth gen i9 CPU, i.e. 9900k, 64 GB RAM
 192 and Nvidia dual RTX 2080 Ti 11 GB VRAM GPUs. Table 2. shows the system specifications.

Table 3. Data Split for Testing / Training & Accuracy Obtained

Dataset (Train/Test) Split in %	Accuracy [%]				
	10 Epochs	20 Epochs	30 Epochs	40 Epochs	50 Epochs
85 – 15	92.31	95.84	96.86	97.39	98.38

193 We first tried to establish the baseline by training a YOLOv3 based detection, For this purpose, we used the
 194 size of input frames as an integer multiple of 32 (416 x 416), with a total of 5 steps for downsampling operation
 195 leading to the largest stride size of 32. As this version used multi-scale analysis, y1,y2 and y3 lead to three
 196 different sizes of feature maps. Information for detection of final bounding boxes comes from the combination of
 197 all three scales. Please see Figure 4 for details. For training, we fine-tune a pre-trained YOLOv3 model, with a
 198 mini-batch size of 32, 10,500 batches, and subdivisions of 15 on 1 GPU, a momentum of 0.8 and a weight decay
 199 of 0.0004. We adopt the multistep learning rate with a base learning rate of 0.0001, and the learning rate scales
 200 of [0.1,0.1].

201 We then designed OYOLO by replacing convolutions by dilated version, For this purpose, we used the size
 202 of input frames as an integer multiple of 32 (416 x 416), without downsampling operation and introduced dilation
 203 rates of 6, 12 and 18 at different levels. The rest of the design remains the same. Information for detection of
 204 final bounding boxes comes from the combination of all three scales. However, the original model size remains
 205 the same as of YOLOv3. We used similar training specifications for our baseline model. Please see Figure 6 for
 206 details.

207 Training and validation loss and accuracy was calculated for our training and validation set—figure 7
 208 displays our training and validation loss. In Figure 7 (a) (b), the accuracy and loss for both training and
 209 testing/validating are presented for each epoch. These graphs were generated for the data split of 85% – 15%.
 210 The accuracy graph visually shows that accuracy for both training and testing increases gradually and then
 211 tends to converge on a specific point. It also shows that after 40 epochs, the change in accuracy reduces as the
 212 validation accuracy appears to be equivalent to training accuracy. Similarly, the right graph shows how the loss
 213 starts decreasing gradually as the model learns on a given dataset. The loss of validation data becomes stable
 214 after 43 epochs and thus tends towards a specific value.

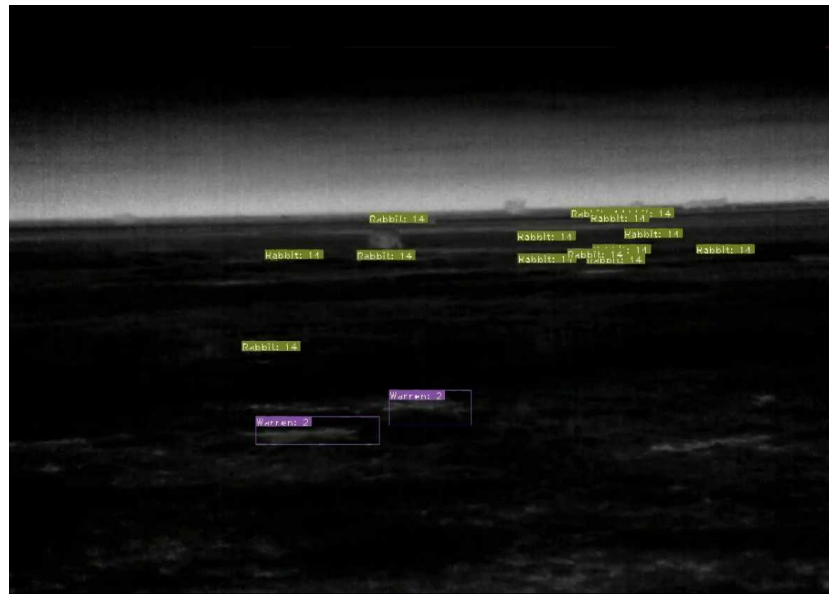


Figure 8. Identification of rabbits and their warrens is shown with their respective labels found by our model. Yellow colour labels belong to rabbits, while purple colour labels are their warrens.

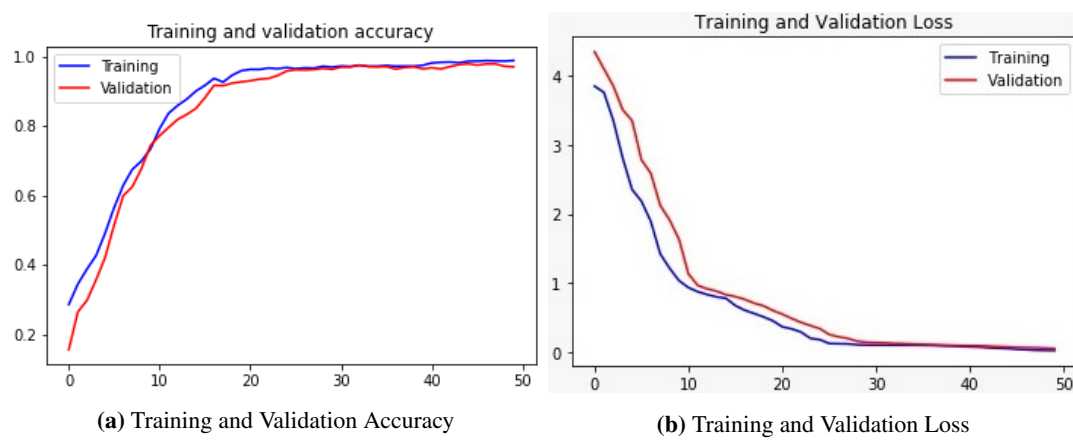


Figure 7. Training and Validation Plots

215 We tested our approach on the data that was not part of our training or validation set. We first detected all
 216 bounding boxes and used them for counting the number of detected pest animals. To remove double counting,
 217 we sustained our count till 10th frame. This value was found empirically based on manual inspection of frames
 218 and detected animals. For verification purposes, we counted ground truth detections and compared with the
 219 automated population count of pest animals. This process also verified our detection results accuracy. Some of
 220 the sample detection results are shown in Figure 10. Detected labels and their sizes are intentionally made small
 221 to show small bounding boxes. Similarly, we also trained our model for automated identification of pest habitats
 222 like rabbit warrens as such places are generally visible in thermal images due to enhanced animal activity in these
 223 regions and their underground presence. Figure 8 Illustrates the detection of rabbits and their warrens.

224 During the testing phase, we achieved an average accuracy of 98.33% for OYOLO compared to 92.33%
 225 accuracy for baseline YOLO model. For Pig class (accuracy = 97.34%, recall = 96.89%, precision = 96.37%
 226 and f1-score = 96.35%) , Rabbit class (accuracy = 98.17%, recall = 96.70%, precision = 96.48% and f1-score =
 227 97.48%) and Kangaroo class (accuracy = 99.48%, recall = 96.96%, precision = 97.30% and f1-score = 98.60%).
 228 Figure 9 visualize the above results. For warren detection, we achieved (accuracy = 93.34%, recall = 96.89%,
 229 precision = 96.37% and f1-score = 96.3%).

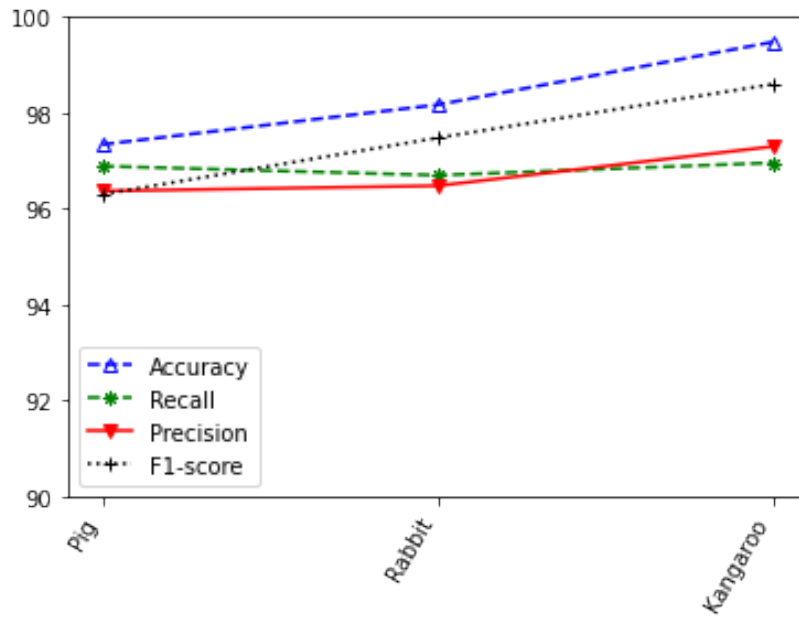


Figure 9. System performance metrics for our proposed system; different metrics are shown for each class of pest animals.

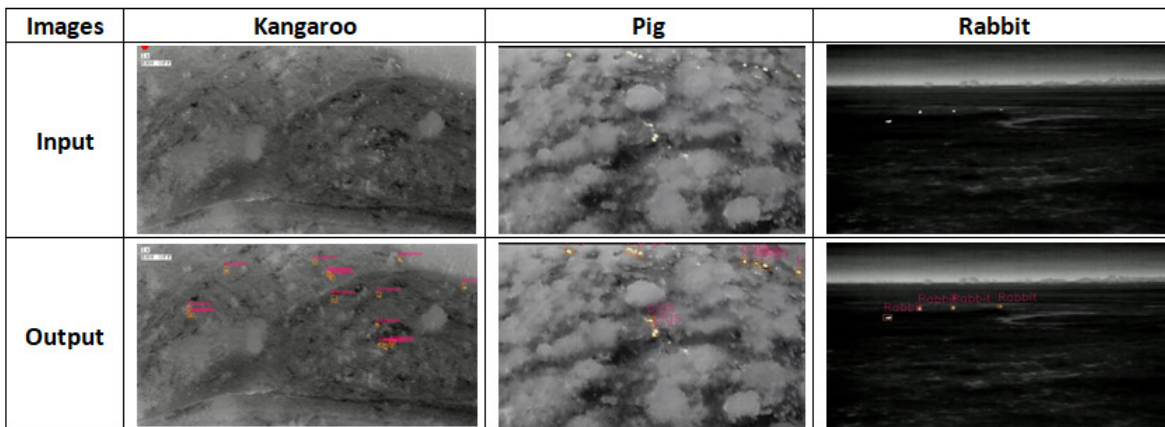


Figure 10. Sample Results: the first row includes input images while the second row shows respective output images. Both bounding boxes and labels are shown.

230 Our system enabled real-time detection of small pest animals in low-resolution video sequences. However,
 231 there are still some weaknesses in our system that we intend to improve in our future work. Our current model
 232 has only trained for three classes of invasive pest animals including pigs, rabbits and Kangaroos. We want to
 233 extend it to include several species of pest animals in our future work. Another aspect that needs improvement is
 234 the removal of double counts as in some instances; the same animal is being counted twice. As accurate count is
 235 not claimed in this paper, we intend to develop some robust strategy to manage this problem in our future work.

236 4. Conclusion

237 In this paper, we proposed a robust and real-time detection system for identification of the potential pests
 238 and their habitat from aerial thermal imaging data. Our dataset had several challenges as the size of target
 239 animals was not only cryptic and small, but the resolution of our cameras was also low. The aim of the project
 240 was to develop a robust system for identification of pest animals in consumer-level cameras. For this purpose, we
 241 optimised the object detection algorithm named YOLO (You Only Look Once) [27] by improving its training and
 242 structure for remote detection of elusive small targets. Our system, trained on the massive data collected from

243 New South Wales and Western Australia, can detect invasive species (rabbits, Kangaroos and pigs) in real-time
244 with a much higher probability of detection compared to the manual detection. This work will facilitate farmers
245 to monitor activities of pest animals in their farmlands.

246 **5. Acknowledgement**

247 This research work is supported by a research grant number 0000102841 by mutually funded by the
248 department of primary industries, New South Wales and department of primary industries and regional
249 development, Western Australia.

250 **References**

- 251 1. Bajiu Mroczkowska, Daniel. 2018. Development of a system for detection, control and prevention of locust pests using
252 uav platforms. B.S. thesis, Universitat Politècnica de Catalunya.
- 253 2. Berg, Amanda, Joakim Johnander, Flavie Durand de Gevigney, Jorgen Ahlberg, and Michael Felsberg. 2019.
254 Semi-automatic annotation of objects in visual-thermal video. In *Proceedings of the IEEE International Conference on
255 Computer Vision Workshops*, pp. 0–0.
- 256 3. Bochkovskiy, Alexey, Chien-Yao Wang, and Hong-Yuan Mark Liao. 2020. Yolov4: Optimal speed and accuracy of object
257 detection. *arXiv preprint arXiv:2004.10934*.
- 258 4. Burke, Claire, Maisie Rashman, Serge Wich, Andy Symons, Cobus Theron, and Steve Longmore. 2019. Optimizing
259 observing strategies for monitoring animals using drone-mounted thermal infrared cameras. *International Journal of
260 Remote Sensing* 40(2), 439–467.
- 261 5. Chen, Guobin, Tony X Han, Zhihai He, Roland Kays, and Tavis Forrester. 2014. Deep convolutional neural network based
262 species recognition for wild animal monitoring. In *2014 IEEE international conference on image processing (ICIP)*, pp.
263 858–862. IEEE.
- 264 6. Corcoran, Evangeline, Simon Denman, Jon Hanger, Bree Wilson, and Grant Hamilton. 2019. Automated detection of
265 koalas using low-level aerial surveillance and machine learning. *Scientific reports* 9(1), 1–9.
- 266 7. Falzon, Greg, Christopher Lawson, Ka-Wai Cheung, Karl Vernes, Guy A Ballard, Peter JS Fleming, Alistair S Glen, Heath
267 Milne, Atalya Mather-Zardain, and Paul D Meek. 2020. Classifyme: a field-scouting software for the identification of
268 wildlife in camera trap images. *Animals* 10(1), 58.
- 269 8. Fleming, Peter JS, Guy Ballard, Nick CH Reid, and John P Tracey. 2018. Invasive species and their impacts on
270 agri-ecosystems: issues and solutions for restoring ecosystem processes. *The Rangeland Journal* 39(6), 523–535.
- 271 9. Gentle, Matthew, Neal Finch, James Speed, and Anthony Pople. 2018. A comparison of unmanned aerial vehicles (drones)
272 and manned helicopters for monitoring macropod populations. *Wildlife Research* 45(7), 586–594.
- 273 10. Georgieva, M, G Georgiev, P Mirchev, E Filipova, et al. 2019. Monitoring on appearance and spread of harmful invasive
274 pathogens and pests in belasitsa mountain. In *X International Agriculture Symposium, Agrosym 2019, Jahorina, Bosnia
275 and Herzegovina, 3-6 October 2019. Proceedings*, pp. 1887–1892. University of East Sarajevo, Faculty of Agriculture.
- 276 11. Girshick, Ross. 2015. Fast r-cnn. In *Proceedings of the IEEE international conference on computer vision*, pp.
277 1440–1448.
- 278 12. Girshick, Ross, Jeff Donahue, Trevor Darrell, and Jitendra Malik. 2014. Rich feature hierarchies for accurate object
279 detection and semantic segmentation. In *Proceedings of the IEEE conference on computer vision and pattern recognition*,
280 pp. 580–587.
- 281 13. GORDON, C. 2001. Sustainable use and pest control in conservation: kangaroos as a case study. *Conservation of
282 exploited species* 6, 403.
- 283 14. Green-Barber, Jai M and Julie M Old. 2019. What influences road mortality rates of eastern grey kangaroos in a
284 semi-rural area? *BMC Zoology* 4(1), 1–10.
- 285 15. Guo, Wei, Weihong Li, Weiguo Gong, and Jinkai Cui. 2020. Extended feature pyramid network with adaptive scale
286 training strategy and anchors for object detection in aerial images. *Remote Sensing* 12(5), 784.
- 287 16. He, Kaiming, Georgia Gkioxari, Piotr Dollár, and Ross Girshick. 2017. Mask r-cnn. In *Proceedings of the IEEE
288 international conference on computer vision*, pp. 2961–2969.
- 289 17. He, Kaiming, Xiangyu Zhang, Shaoqing Ren, and Jian Sun. 2016. Deep residual learning for image recognition. In
290 *Proceedings of the IEEE conference on computer vision and pattern recognition*, pp. 770–778.

291 18. Jepsen, Emma M, André Ganswindt, Celiwe A Ngcamphalala, Amanda R Bourne, Amanda R Ridley, and Andrew E
292 McKechnie. 2019. Non-invasive monitoring of physiological stress in an afrotropical arid-zone passerine bird, the southern
293 pied babbler. *General and Comparative Endocrinology* 276, 60–68.

294 19. Kellenberger, Benjamin, Diego Marcos, Sylvain Lobry, and Devis Tuia. 2019. Half a percent of labels is enough:
295 Efficient animal detection in uav imagery using deep cnns and active learning. *IEEE Transactions on Geoscience and*
296 *Remote Sensing* 57(12), 9524–9533.

297 20. Lin, Tsung-Yi, Piotr Dollár, Ross Girshick, Kaiming He, Bharath Hariharan, and Serge Belongie. 2017. Feature pyramid
298 networks for object detection. In *Proceedings of the IEEE conference on computer vision and pattern recognition*, pp.
299 2117–2125.

300 21. Lin, Tsung-Yi, Michael Maire, Serge Belongie, James Hays, Pietro Perona, Deva Ramanan, Piotr Dollár, and C Lawrence
301 Zitnick. 2014. Microsoft coco: Common objects in context. In *European conference on computer vision*, pp. 740–755.
302 Springer.

303 22. Liu, Mingjie, Xianhao Wang, Anjian Zhou, Xiuyuan Fu, Yiwei Ma, and Changhao Piao. 2020. Uav-yolo: Small object
304 detection on unmanned aerial vehicle perspective. *Sensors* 20(8), 2238.

305 23. Liu, Wei, Dragomir Anguelov, Dumitru Erhan, Christian Szegedy, Scott Reed, Cheng-Yang Fu, and Alexander C Berg.
306 2016. Ssd: Single shot multibox detector. In *European conference on computer vision*, pp. 21–37. Springer.

307 24. Meek, Paul D, Guy-Anthony Ballard, Karl Vernes, and Peter JS Fleming. 2015. The history of wildlife camera trapping
308 as a survey tool in australia. *Australian Mammalogy* 37(1), 1–12.

309 25. Meena, Divya and L Agilandeswari. 2020. Invariant features-based fuzzy inference system for animal detection and
310 recognition using thermal images. *International Journal of Fuzzy Systems*, 1–12.

311 26. Redmon, Joseph, Santosh Divvala, Ross Girshick, and Ali Farhadi. 2016. You only look once: Unified, real-time object
312 detection. In *Proceedings of the IEEE conference on computer vision and pattern recognition*, pp. 779–788.

313 27. Redmon, Joseph and Ali Farhadi. 2017. Yolo9000: better, faster, stronger. In *Proceedings of the IEEE conference on*
314 *computer vision and pattern recognition*, pp. 7263–7271.

315 28. Redmon, Joseph and Ali Farhadi. 2018. Yolov3: An incremental improvement. *arXiv preprint arXiv:1804.02767*.

316 29. Ren, Shaoqing, Kaiming He, Ross Girshick, and Jian Sun. 2015. Faster r-cnn: Towards real-time object detection with
317 region proposal networks. In *Advances in neural information processing systems*, pp. 91–99.

318 30. Sejnowski, Terrence J. 2018. *The deep learning revolution*. Mit Press.

319 31. Shepley, Andrew Jason, Greg Falzon, Paul Meek, and Paul Kwan. 2020. Location invariant animal recognition using
320 mixed source datasets and deep learning. *bioRxiv*.

321 32. van Hespen, Rosanna, Cindy E Hauser, Joe Benshemesh, Libby Rumpff, and José J Lahoz Monfort. 2019. Designing a
322 camera trap monitoring program to measure efficacy of invasive predator management. *Wildlife Research* 46(2), 154–164.

323 33. West, Peter and Glen Saunders. 2003. Pest animal survey 2002. *An analysis of pest animal distribution and abundance*
324 *across NSW and the ACT. NSW Agriculture, Orange*.

325 34. Yu, Fisher and Vladlen Koltun. 2015. Multi-scale context aggregation by dilated convolutions. *arXiv preprint*
326 *arXiv:1511.07122*.

327 35. Yu, Fisher, Vladlen Koltun, and Thomas Funkhouser. 2017. Dilated residual networks. In *Proceedings of the IEEE*
328 *conference on computer vision and pattern recognition*, pp. 472–480.